PERFORMANCE EVALUATION AND OPTIMIZATION OF AN ULTRASONIC SPRAY ATOMIZERS SYSTEM FOR HVAC APPLICATIONS

Navarro P., Ruiz J.*, Lucas M., Martínez P., Pérez J., Rodrígez A.
*Author for correspondence
Departamento de Ingeniería Mecánica y Energía
Universidad Miguel Hernández
Avda. de la Universidad s/n, 03202 Elche, Spain
E-mail: j.ruiz@umh.es

ABSTRACT

One of the techniques that is currently being developed to improve the efficiency of air conditioning equipment is using evaporative cooling to pre-cool the air that reaches the condenser of a refrigeration machine. Previous works studied the use of an ultrasonic mist generator and obtained promising results. However, the mist generator has some limitations, as not being able to control the distribution and size of the droplets. The main objective of this work has been to develop a numerical model of an ultrasonic spray atomizer that overcomes these limitations.

The spray injection has been modified depending on the different arrangements of the spray atomizer studied. The commercial code ANSYS FLUENT will be used to numerically solve the governing equations. A parametric analysis has been carried out considering the most important variables in the cooling process: the effect of the ultrasonic frequency, the injected water mass flow rate, the droplet size, the cooled area and the energy consumption. Based on these variables, the optimal combination aims to obtain the highest cooling rate. It has been interesting to explore the influence of the number of injections and their location. Experimentally this is complex, but from the CFD it can be configured easily. In view of the results, the performance increases when the number of injections, the droplet size and the humidity of the inlet air increase, and when the temperature of the inlet air decreases. The maximum COP for all the simulations studied was 7.40, for 81 injections, D_d=10μm, T_∞=25ºC and ϕ_∞=70 %.

NOMENCLATURE

Symbols

A_d	[m^2]	area of the droplet
A_T^x	[-]	percentage area for temperature T, at section x
b	[m]	domain width
C_D	[m]	drag coefficient
c_p	[J kg^{-1} K^{-1}]	specific heat at constant pressure
D_d	[m]	droplet diameter
g	[m s^{-2}]	gravitational constant
h	[m]	domain height
L	[m]	domain length
L_w	[m]	wet length
l	[m]	distance between inlet sections
$\dot{m}_w$	[kg$_w$ s^{-1}]	mass flow rate of spray atomizers
Nu	[-]	Nusselt number
Pr	[-]	Prandtl number
$\dot{Q}_{\text{cooling}}$	[W]	cooling capacity
Re	[-]	Reynolds number
T	[°C]	dry temperature
T_{wb}	[°C]	wet bulb temperature
$\bar{T}^x$	[°C]	mean temperature calculated at section x
$\dot{W}_{\text{ultrasound}}$	[W]	power absorbed by spray atomizers

Greek symbols

$\bar{\eta}^x$	[-]	evaporative cooling efficiency calculated at section x
μ	[kg m^{-1} s^{-1}]	dynamic viscosity
ϕ	[-]	relative humidity
ρ	[kg m^{-3}]	density
τ	[kg m^{-3}]	stress tensor
Re	[-]	Reynolds number

Subscripts

a	air
d	droplet
∞	ambient conditions
ma	moist air
w	water

Abbreviations

CFD	computational fluid dynamics
COP	coefficient of performance
HVAC	heating, ventilation and air-conditioning

INTRODUCTION

The energy consumption used in buildings around the world today in air conditioning systems or electric fans to stay cool accounts almost 20% of their total electricity consumption. This further development will have implications for countries' overall energy demand, putting pressure on electricity grids and increasing local and global emissions, [1]. An answer to achieve a more sustainable path necessarily involves the use of renewable energy and the use of very efficient technologies.

Evaporative cooling techniques applied to the condenser of a refrigerating machine represent one of the most effective and immediately applicable solutions for improving the efficiency of domestic and commercial air conditioning systems worldwide.

Applications of ultrasonic energy to enhance a wide variety of processes or to improve system efficiency have been explored in recent years. [2] made an overview of studies about the applications of ultrasound as a new technology in the field of Heating, Ventilation and Air-Conditioning (HVAC). They claimed that, from a general point of view, all the effects produced by ultrasound could be interesting in applications involving heat or mass transport, decreasing both the external and internal resistance to transport. Recently, [3] presented a review of the state-of-the-art of high-intensity ultrasound and its applications. However, the authors did not specifically cite evaporative cooling as an application of ultrasound, denoting the little attention they have received to date.

Computational Fluid Dynamics (CFD) techniques enables scientists and designers to understand the physical principles of spraying processes saving time and effort in tedious experimental work. Literature review shows that several authors face the analysis of spray cooling for different applications using CFD models. For example, [6] showed the possibility of using saline water for pre-cooling the inlet air to a heat exchanger. They develop a CFD model to predict the wet length of saline water droplets in spray cooling for different ambient conditions and spray characteristics.

However, although it has been possible to study several cases of CFD simulations of droplet spraying for pre-cooling, few references have been found in the bibliographic review related to the numerical simulation of ultrasonic mist generators, and none of them was related to the evaporative pre-cooling of the inlet air of the condenser in air conditioning applications. Recently, [7] numerically simulated a ultrasonic gas atomizer. Through numerical simulation, they decided generation position and operating conditions of ultrasound atomizer.

As last references, there would be the previous works of this research group. Martinez et al. [10] shows the design and the first tests in a ultrasonic mist generation. Its thermal performance and its water mist production capacity were assessed in terms of the mass flow rate of atomized water and size distribution of the droplets generated. For the design of the prototype and based on the experimental data collected, a numerical model was developed in CFD. Which made it possible to carry out parametric studies to know the effect that certain operating variables had on the cooling capacity and the distribution of the generated mist, Ruiz et al. [8]. Although the tests were satisfactory and their scientific interest has been revealed by the recent publications achieved, there are still many aspects related to the search for the optimal design of the pre-cooling system based on ultrasound techniques and its integration into commercial equipment. The main modification proposed is the change in the droplet generation system, if in the cited works a mist generator was used, in the current study the use of ultrasonic spray atomizers is proposed.

In conclusion, the works referring to the precooling of the inlet air with ultrasonic atomization techniques have been reviewed and it has been observed that this technique has received limited attention for this application, with few references found in the literature to date. Despite this, it has been proven that ultrasound is a promising method to improve the design of evaporative precooling systems. Therefore, the main objective of this study will be to develop a numerical model of an ultrasonic spray atomizers system. The objective is the optimization of the pre-cooling system taking into account its key operating parameters: maximizing evaporative efficiency, increasing the useful area and reducing the wet length.

MATERIALS AND METHODS

Experimental test facility

To obtain key parameters that will be used in the simulations, a series of experimental tests have been carried out with the ultrasonic spray atomizers that will be used in the future in the experimental prototype. The test equipment mainly consists of two components: a ultrasonic spray atomizers system and a wind tunnel.

The device used in the system is a hybrid mesh and ultrasound spray atomizer (Figure 1). This is composed of a ceramic piezoelectric, which surrounds a porous membrane, and a PCB controller board that generates a pulse signal at a frequency of 108 kHz for the spray atomizer. This component is characterized by having a low cost and consumption (2W).

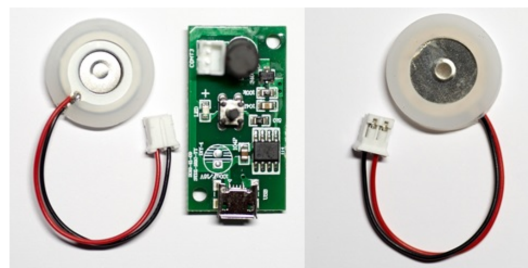

Figure 1. Used ultrasonic spray atomizers.

When the current is supplied, the piezoelectric initiates an expansion/contraction cycle, this oscillation allows the water to pass through its microscopic holes (around an opening of 10 μm, Figure 2) , and pushes the drops forming a column of water mist. The mass flow rate is approximately 8.33x10^{-6} kg$_w$ s^{-1}.

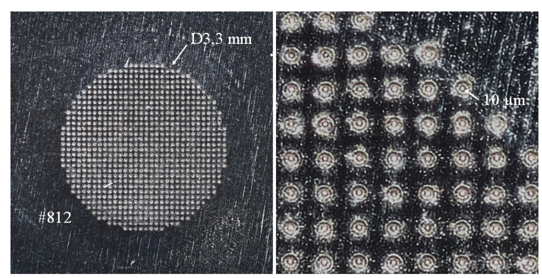

Figure 2. Microscopic image of the water outlet holes in the spray atomizers used.

In order to characterize the real geometry of the spray atomizer discs and the dimensions of the nebulized drops, with the aim of making a numerical model as close as possible to reality, it was decided to adopt the photographic techniques described in [10]. An example of these is shown in Figure 3.

As for how the working frequency affects the operation of the spray atomizers. In Yan et al. [9] a study of the influencing factors in the atomization flow of a mesh piezoelectric transducer was carried out. If we focus on the results obtained for the tests in which the frequency was modified, it was observed that the frequency notably affects the mass output of the spray atomiz-

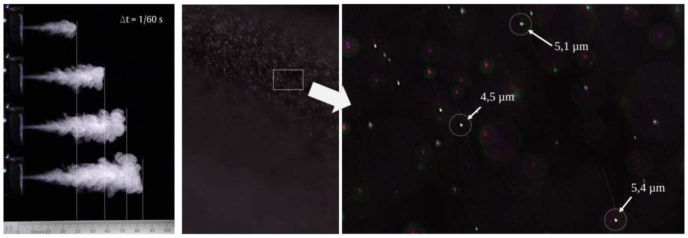

(a) (b)

Figure 3. Experimental test carried out to define: (a) the speed of exit of the drops, and (b) the output size of the drops.

ers, obtaining the maximum flow point at 122 kHz for the spray atomizers used in this study. In our case, the spray atomizers are powered by a PCB driver board that generates a pulse signal at a frequency of 108 kHz, which cannot be modified.

Physical model

The physical domain considered in the simulations reproduces a portion of the experimental facility where the future tests will be performed. It consists of a 2.5 m long, 0.492 m wide and 0.712 m high ($L \times b \times h$) domain (Figure 4). The water spray injections will be located at certain points of the air inlet section and in the direction of the air outlet section. The reason is that it will be there where the manifold will be located where the spray atomizers will be installed (Figure 5). These are included in a square of 0.35×0.35 m^2.

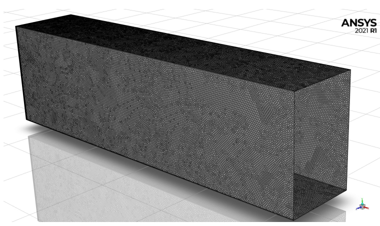

Figure 4. Wind tunnel domain considered in the simulations and boundary conditions.

Mathematical method (governing equations)

Continuous phase (moist air)

The airflow was assumed to be steady, incompressible and turbulent flow. The Reynolds-Averaged Navier-Stokes equations (RANS) were used along the standard k-ε turbulence model. No turbulence model can be considered superior than the others [5], but the standard k-ε turbulence model has been reported to accurately predict the flow field and droplet evaporation in several spray cooling applications [4]. The influence of water droplets on the airflow was considered by introducing the source terms of mass, momentum and energy into the air-side governing equations. In spray cooling applications, heat, mass and momentum is transferred between the moist, unsaturated air stream and the water droplets. Processes related to heat-and-mass transfer between different phases are governed by mass, momentum, energy and species conservation principles. This multiphase flow is described by the set of equations that governs the continuous phase (internal moist air inside the wind tunnel) and the set of equations for the discrete phase (ultrasound-generated water droplets). The continuous and discrete phase equations are coupled by the source terms of the conservation equations. In this study, an Eulerian–Lagrangian approach was used.

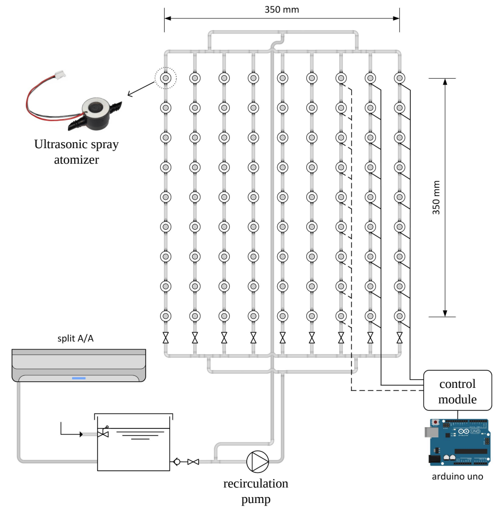

Figure 5. Scheme of the distribution of the spray atomizers in the form of a 9x9 manifold.

$$\frac{\partial(\rho v_i)}{\partial x_j} = S_m \tag{1}$$

$$\frac{\partial(\rho v_i v_j)}{\partial x_j} = -\frac{\partial p}{\partial x_i} + \frac{\partial \tau_{ij}}{\partial x_j} + \rho g_i + S_{mo} \tag{2}$$

$$\rho v_i \frac{\partial e}{\partial x_j} = -p\frac{\partial v_i}{\partial x_j} + \frac{\partial}{\partial x_j}\left(k\frac{\partial T}{\partial x_j}\right) + \frac{\partial}{\partial x_j}\left(\sum_{i'=1}^{n} h_{i'} J_{i'}\right) + \phi_v + S_e \tag{3}$$

$$\rho v_i \frac{\partial m_j}{\partial x_j} = -\frac{\partial J_{i',i}}{\partial x_j} + S_m \tag{4}$$

$$J_{i',i} = -\rho D_{f_{i',m}} \frac{\partial m_j}{\partial x_j} \tag{5}$$

Here, S_m, S_{mo}, S_e represent the mass, momentum and energy source terms introduced by water droplets, respectively, and $J_{i',i}$ is the diffusion flux of species i'.

Discrete phase

The equations for the spherical water droplets are written in a Lagrangian reference frame. The trajectory of a discrete phase particle is obtained by integrating the force balance on the droplet (Newton's second law of motion),

$$\frac{dv_d}{dt} = \frac{18\mu}{\rho_d d_d^2}\frac{C_D \mathrm{Re}}{24}(v - v_d) + g\frac{\rho_d - \rho}{\rho_d} \tag{6}$$

$$\frac{dr_d}{dt} = v_d \tag{7}$$

The drag coefficient (C_D) included in the the drag per unit droplet mass term can be calculated as reported by [11].

Due to the existence of a temperature difference and a vapour concentration gradient between the water droplets and the unsaturated air, heat and mass transfer between them occur. The energy conservation equation of a droplet, neglecting the radiation effect, is expressed as,

$$m_d c_p \frac{dT_d}{dt} = h_C A_d (T - T_d) + \frac{dm_d}{dt} h_{fg} \tag{8}$$

It relates the temperature change in the droplet to the convective and latent heat transfer between the droplet and the continuous phase. The rate of evaporation of water changes according to,

$$\frac{dm_d}{dt} = h_D A_d M (y_s - y) = h_D A_d (\rho_s - \rho) \tag{9}$$

The convective and mass transfer coefficients (h_C, h_D) are calculated from the Nusselt and Sherwood number correlations reported by [12],

$$\mathrm{Nu} = \frac{h_C d_d}{k} = 2 + 0.6 \mathrm{Re}_d^{1/2} \mathrm{Pr}^{1/2} \tag{10}$$

$$\mathrm{Sh} = \frac{h_D d_d}{D_f} = 2 + 0.6 \mathrm{Re}_d^{1/2} \mathrm{Sc}^{1/2} \tag{11}$$

Numerical method

The boundary conditions used in the present analysis are shown in Figure 4. Air enters the computational domain at the leftmost surface shown in the figure. It is in this section that the water injections are located. In Figure 3(a) it can be seen as the flow that there is a lot of turbulence in the dispersion of the particles, this has been introduced in the RANS model using a stochastic tracking model referred as Discrete Random Walk in ANSYS FLUENT. The turbulent dispersion of droplets is predicted by integrating the trajectory equations for individual particles, using the instantaneous fluid velocity along the particle path during the integration. By computing the trajectory for a sufficient number of representative particles (tries), the random effects of turbulence on the particle dispersion may be simulated. Therefore the number of particles that we introduce will be multiplied by 5.

The inlet air speed conditions have been considered uniform and an air speed of 1.5 m s^{-1} has been set. A turbulence intensity of 5% was assumed for the inflows [13]. The incoming spray water was adjusted to match what was measured. To establish the injection speed of the continuous phase, experimental measurements were made, as shown in Figure 3(a). It is around 2.5 m s^{-1}. On the other hand, the droplet temperature was set equal to the air temperature used in each simulation. The pressure was stated to be equal to the ambient pressure at the outlet section (pressure outlet). Wall boundary condition was selected for the tunnel walls. The zero heat flux and no-slip condition were imposed on them. The 'escape' boundary condition was set, meaning that the droplets exit the computational domain when they reach the walls or the tunnel exit [4]. For droplet size distribution, different droplet sizes have been studied (5 μm and 10μm). These correspond to the size of the drops generated by the spray atomizer (Figure 3(b)) and the size of the drops generated by the mist generator used in previous works [8] respectively.

The commercial code ANSYS FLUENT (version 19.1) was utilised to numerically solve the governing equations.

The selected grid is an unstructured grid with 770,317 polyhedral cells. This will be the same for all analysis. The SIMPLE algorithm was employed to solve the coupling between continuity and momentum equations through pressure. All calculations were performed using discretization providing second order accuracy. The convergence criterion in each case was $|\varphi(i+1) - \varphi(i)|/\varphi(i) < 10^{-4}$, where i denotes the iteration number and φ can stand for any of the dependent variables.

RESULTS AND DISCUSSION

Parametric analysis

A parametric study was conducted to analyze the influence of some operating variables in the evaporative performance of the ultrasonic generator. The conditions used and the configuration described in the section are the same as those used in previous works [8]. More information about the model validation process can be found here.

The variables included (Table 1) in this study were: number and layout of the injection flow, droplet diameter. In addition to environmental conditions such as temperature and air humidity.

Distribution	Nº injections	D_d (μm)	T_∞(ºC)	ϕ_∞(%)
9x9	81	5	25	50
9x9 - F=1,3,5,7,9	45	10	30	70

Table 1. Conditions studied.

As can be seen in the Table 1, 2 types of distribution were studied, which have been selected based on the distribution that the experimental installation will subsequently have (Figure 5). The spray atomizers must be working whenever water reaches them, otherwise they generate dripping. Therefore, the tested cases are activating the 9 rows (9x9) and another activating 5 (9x9 - F=1,3,5,7,9).

The droplet sizes studied were 5μm and 10μm, as explained in the section . Finally, for the environmental conditions, 2 levels of both temperature and humidity were studied. Therefore, the total number of simulations carried out was 16. The rest of the variables involved in the parametric analysis were considered constant.

The evaporative cooling efficiency at the certain section, $\bar{\eta}^x$, is defined as the ratio of the mean temperature difference calculated at the evaluated section, $T_\infty - \bar{T}^x$, to the wet bulb depression ($T_\infty - T_{wb_\infty}$).

$$\bar{\eta}^x = \frac{T_\infty - \bar{T}^x}{T_\infty - T_{wb_\infty}} \tag{12}$$

Figure 6 shows the evaporative cooling efficiency evaluated in the outlet section of the domain, $\bar{\eta}^L$, as a function of the air inlet temperature for all the simulations performed.

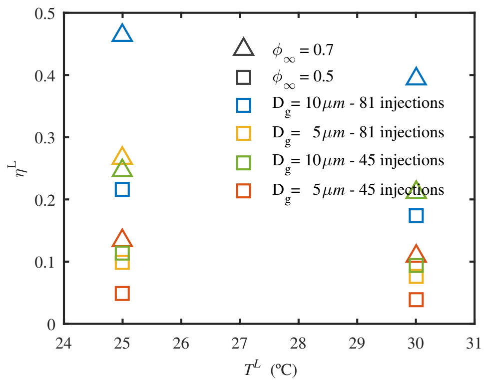

Figure 6. Evaporative cooling efficiency as a function of the water temperature for all simulations conducted.

As can be seen, the results are scattered over a wide range from $\bar{\eta}^L = 0.038$ to 0.464. The maximum efficiency of $\bar{\eta}^L = 0.464$ is given for the case of 81 injections, D_d=10μm, T_∞=25ºC and ϕ_∞=70%.

The trend observed for all the results is that the efficiency increases with a greater number of injections. This is logical, since the greater the number of injections, the mass flow rate of water increases. Efficiency also increases with increasing D_d. This is because as D_d increases, the droplets evaporate more slowly and therefore the wet lengths are greater (as will be seen later). Finally, higher humidity and lower air temperature also improve efficiency. This is directly related to the wet bulb temperature.

The evaporative cooling efficiency gives an overall representation of the cooling processes taken place in the domain since is referred to the mean temperature. However, this magnitude fails may not be able to represent local effects.

To perform a quantitative comparison between the studied cases, the difference between the maximum, mean and minimum temperatures for the 16 tests was studied. Where it was observed that the temperatures are very close to each other (maximum difference is 0.53%). Therefore, the average temperature is a representative value for all outlet section. This can also be seen in Figure 7(a),(c) and (e).

The last indicator discussed in this section is the wet length, L_w. The wet length is the distance from the droplet injection section until the water droplets completely evaporate. This phenomenon can cause corrosion, scaling and fouling on the heat exchanger bundles if not fully evaporated water droplets are carried out by the airstream to the heat exchanger bundles of the condenser.

The wet length (in its dimensionless form, L_w/L) is shown in Figure 8. As can be seen, in none of the simulated cases is it greater than unity, which means that no drop leaves the domain through the outlet section. The wet length depends on all the parameters, although mainly on the number of injections and the diameter of the drops, since the higher the mass flow rate of water

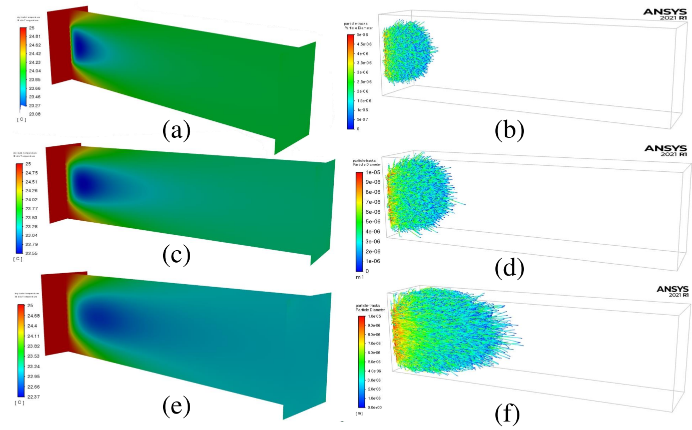

Figure 7. Temperature contours in the axial mid plane and the outlet section of the domain (a,c,e) and evolution of the diameter of the drops from when they leave the spray atomizers until they completely evaporate (b,d,f) for the tests of 81 injection, T_∞ = 25 ºC: (a,b) D_d=5μm y $\phi_\infty = 0.7$; (c,d) D_d=10μm y $\phi_\infty = 0.5$; and (e,f) D_d=10μm y $\phi_\infty = 0.7$.

and the larger the drops, they take longer to evaporate. It also increases with humidity and temperature. As an example, Figure 7 shows the prediction of drop trajectories in three representative cases.

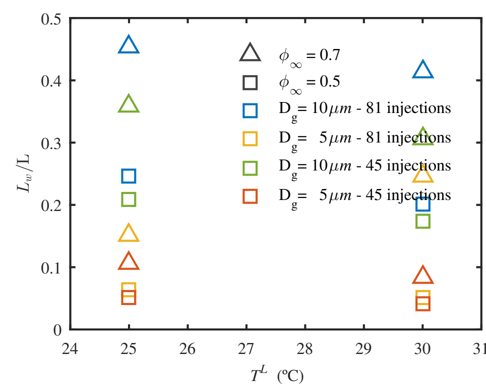

Figure 8. Wet length (in its dimensionless form, L_w/L) as a function of water temperature for all simulations performed.

This allows identifying the minimum length at which to locate the spray atomizers of condenser. For the cases studied, the minimum length is 1.137 m. However, if it is planned to work with humidities above 70%, a greater $\dot{m}_w$, or a greater diameter of drops, should be studied. This ensures that the installation always works in ranges where complete evaporation occurs.

Optimization analysis

From the above discussion, it has been highlighted that an increase of $\dot{m}_w$, increases the cooling efficiency, at least, until the saturation is reached. However, this will imply having to introduce a greater number of spray atomizers and a higher energy consumption (2W/spray atomizer). Under these conditions, the cooling capacity, $\dot{Q}_{\text{cooling}}$, defined as in Equation (13), is also increased due to the temperature difference (via the cooling efficiency).

$$\dot{Q}_{\text{cooling}} = \dot{m}_a c_{p_a} \left(T_\infty - \bar{T}^L\right) \tag{13}$$

Considering these, the relative contribution of all these effects can be seen in the coefficient of evaporative performance (COP), Equation (14):

$$\text{COP} = \frac{\dot{Q}_{\text{cooling}}}{\dot{W}_{\text{ultrasound}}} \tag{14}$$

Figure 9 presents the variation of the performance coefficient against the air inlet temperature for all the simulations carried out. As can be seen, despite the increase in consumption, the increase in injections always improves the COP, although not very significantly. Moreover, in general terms, the COP decreases with increasing air temperature and increases with increasing humidity and droplet size.

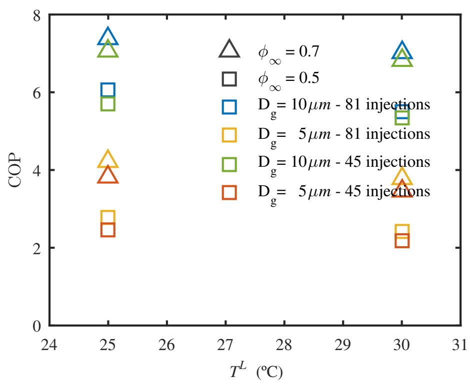

Figure 9. Performance coefficient depending on the water temperature for all the simulations carried out.

CONCLUSIONS

In this article, a numerical model of an ultrasonic spray atomizer system for evaporative pre-cooling of condenser inlet air in air conditioning applications has been developed. A parametric analysis including some physical variables involved in the cooling process was carried out (number and distribution of injections, droplet diameter, and air temperature and humidity). Finally, an optimization study regarding the overall cooling performance, for the above mentioned application, was performed. The main conclusions obtained during this investigation can be summarized as follows.

The average evaporative cooling efficiency evaluated in the output section of the domain, $\bar{\eta}^L = 0.464$, increases when the number of injections, droplet size and humidity increase, and when the temperature decreases. The maximum value is $\bar{\eta}^L$=0.464 and is given for 81 injections, D_d=10μm, T_∞=25ºC and ϕ_∞=70%.

The observations regarding the wet length have allowed us to know that the distribution of is quite homogeneous. As well as the minimum length at which to locate the spray atomizers of condenser. The most unfavorable moisture length is L_w/L=0.455 and is given for the case of 81 injections, D_d=10μm, $T_\infty = 25$ ºC and $\phi_\infty = 70\%$.

The optimization analysis based on the coefficient of performance has shown that the operating ranges that show better overall performance are the same as for the previous cases (81 injections, D_d=10μ m, T_∞=25ºC and ϕ_∞=70%) and is 7.40. For these conditions, there is a greater wet length and this, together with the rest of the factors, favors the evaporative process. However, as already mentioned, having a very large wet length can be a problem, so both factors must be taken into account when designing the prototype.

REFERENCES

[1] IEA. *The Future of Cooling: Opportunities for Energy-Efficient Air Conditioning*; Annual report; IEA: Paris, France, 2018.

[2] Research and applications of ultrasound in HVAC field: A review. *Renewable and Sustainable Energy Reviews*, Vol. 58, 2016, pp. 52–68

[3] Yao, Y.; Pan, Y.; Liu, S. Power ultrasound and its applications: A state-of-the-art review. *Ultrasonics Sonochemistry*, Vol. 62, 2020, pp. 104722

[4] Alkhedhair, A.; Gurgenci, H.; Jahn, I.; Guan, Z.; He, S. Numerical simulation of water spray for pre-cooling of inlet air in natural draft dry cooling towers *Applied Thermal Engineering*, Vol. 61, 2013, pp. 416-424

[5] Montazeri, H.; Blocken, B.; Hensen, J. Evaporative cooling by water spray systems: CFD simulation, experimental validation and sensitivity analysis. *Building and Environment*, Vol. 83, 2015, pp. 129–141

[6] Sadafi, M.; Ruiz, J.; Lucas, M.; Jahn, I.; Hooman, K. Numerical and experimental study on a single cone saline water spray in a wind tunnel. *International Journal of Thermal Sciences*, Vol. 120, 2017,pp. 190–202

[7] Kim, K.D.; Jin, D.H.; Choi, Y.C. Numerical simulation on the generation of ultrasound and formation of water fog in the ultrasonic gas atomizer. *Ultrasonics*, Vol. 102, 2020, pp. 105851

[8] Ruiz, J.; Martínez, P.; Martín, Í.; Lucas, M. Numerical Characterization of an Ultrasonic Mist Generator as an Evaporative Cooler. *Energies*, Vol. 13, 2020, pp. 2971

[9] Yan Q, Sun W, Zhang J. Study on the Influencing Factors of the Atomization Rate in a Piezoceramic Vibrating Mesh Atomizer. *Applied Sciences*, Vol. 10(7), 2020, pp. 2422

[10] Martinez, P.; Ruiz, J.; Martin, I.; Lucas, M. Experimental study of an ultrasonic mist generator as an evaporative cooler. *Applied Thermal Engineering*, Vol. 181, 2020, pp. 116057

[11] Morsi, S.A.; Alexander, A.J. An investigation of particle trajectories in two-phase flow systems. *Journal of Fluid Mechanics*, Vol. 55, 1972, pp. 193–208

[12] Ranz, W.E.; Marshall, W.R. Evaporation from drops part I. *Chemical Engineering Progress*, Vol. 48, 1952, pp. 141–146

[13] Ruiz, J.; Kaiser, A.; Zamora, B.; Cutillas, C.; Lucas, M. CFD analysis of drift eliminators using RANS and LES turbulent models. *Applied Thermal Engineering*, Vol. 105, 2016, pp. 979–987